The Astrophysical Journal, 962:190 (10pp), 2024 February 20 https://doi.org/10.3847/1538-4357/ad1883

Discrepancies in the Properties of a Coronal Mass Ejection on Scales of 0.03 au as Revealed by Simultaneous Measurements at Solar Orbiter and Wind: The 2021 November 3–5 Event

F. Regnault[1], N. Al-Haddad[1], N. Lugaz[1], C. J. Farrugia[1], W. Yu[1], B. Zhuang[1], and E. E. Davies[2]
[1] Space Science Center, Institute for the Study of Earth, Oceans, and Space, University of New Hampshire, USA; florian.regnault@unh.edu
[2] Austrian Space Weather Office, GeoSphere Austria, Graz, Austria
Received 2023 September 18; revised 2023 December 6; accepted 2023 December 21; published 2024 February 20

Abstract

Simultaneous in situ measurements of coronal mass ejections (CMEs), including both plasma and magnetic field, by two spacecraft in radial alignment have been extremely rare. Here, we report on one such CME measured by Solar Orbiter (SolO) and Wind on 2021 November 3–5, while the spacecraft were radially separated by a heliocentric distance of 0.13 au and angularly by only 2.2°. We focus on the magnetic cloud (MC) part of the CME. We find notable changes in the *R* and *N* magnetic field components and in the speed profiles inside the MC between SolO and Wind. We observe a greater speed at the spacecraft farther away from the Sun without any clear compression signatures. Since the spacecraft are close to each other and computing fast magnetosonic wave speed inside the MC, we rule out temporal evolution as the reason for the observed differences, suggesting that spatial variations over 2.2° of the MC structure are at the heart of the observed discrepancies. Moreover, using shock properties at SolO, we forecast an arrival time 2 hr 30 minutes too late for a shock that is just 5 hr 31 minutes away from Wind. Predicting the north–south component of the magnetic field at Wind from SolO measurements leads to a relative error of 55%. These results show that even angular separations as low as 2.2° (or 0.03 au in arc length) between spacecraft can have a large impact on the observed CME properties, which raises the issue of the resolutions of current CME models, potentially affecting our forecasting capabilities.

Unified Astronomy Thesaurus concepts: Solar coronal mass ejections (310); Heliosphere (711)

1. Introduction

The launch of Solar Orbiter (SolO; Müller et al. 2020) and of Parker Solar Probe (PSP; Fox et al. 2016; Raouafi et al. 2023) enable measurements of coronal mass ejections (CMEs) in the innermost heliosphere at heliocentric distances below 0.5 au. Combined with older missions around 1 au, such as Wind, the Advanced Composition Explorer (ACE; Chiu et al. 1998), the Deep Space Climate Observatory (Burt & Smith 2012), and the Solar Terrestrial Relations Observatory (STEREO-A/B; Kaiser & Adams 2007; Kaiser et al. 2008), these measurements provide opportunities to study CMEs using multiple spacecraft distributed at different distances from the Sun. Such multi-spacecraft studies have so far focused on two main approaches depending on the distance between the spacecraft. The first combines simultaneous measurements by two spacecraft within the CME, i.e., at the same time but at different locations, often with moderate (typically ∼10°–20°) angular separations in longitude, to investigate the three-dimensional nature of CME properties, as done, for example, by Winslow et al. (2021). This particular study relied on measurements from STEREO-A and PSP near 1 au, a location where PSP does not typically provide full plasma measurements. Because SolO performed Earth flybys, the mission has been making solar wind plasma and interplanetary magnetic field measurements close to the Sun–Earth line and at distances of 0.5–1 au. The second approach relies on combining distant measurements from two spacecraft in approximate radial alignment to investigate CME propagation and evolution (see, e.g., Davies et al. 2021b; Kilpua et al. 2021; Möstl et al. 2022) for CMEs first measured by SolO at a heliocentric distance of 0.8 au. Other studies before the launches of PSP and SolO used measurements in the inner heliosphere from planetary missions such as MESSENGER and Venus Express (see, e.g., Winslow et al. 2015; Good & Forsyth 2016; Salman et al. 2020; Lugaz et al. 2022), which do not have plasma measurements. Earlier work used measurements from the Helios probes (see, e.g., Leitner et al. 2007; De Lucas et al. 2011) in the 1980s, but data quality and the lack of remote observations made reaching global conclusions more complicated. Regarding recent work with SolO, Davies et al. (2021b) studied a CME measured on 2020 April 19–21 by SolO, BepiColombo, and Wind while SolO was at 0.81 au, but no plasma measurements were available at SolO because the Solar Wind Analyser (SWA) suite commissioning was still ongoing. There was notable evolution of the CME between SolO and Wind, with a decrease of the magnetic field strength in the flux rope by ∼35% and an increase in duration by 10%–15%. Importantly, measurements of the flux rope at Wind (on April 20, 07:56 UT) started just 1 hr before the end of the flux rope at SolO (April 20, 09:15 UT). Thus, a small portion of these measurements were made simultaneously at two spacecraft locations, and any discrepancies found may be thought more as the temporal evolution of the CME during the time it takes to pass over SolO rather than the effect of CME propagation from SolO to Wind.

In this paper, we focus on a CME measured by SolO and Wind on 2021 November 3–5 while they were separated by 0.13 au in heliocentric distance (Wind was at 0.98 au and SolO at 0.85 au from the Sun) and for which both spacecraft provided plasma and magnetic field measurements. Their total

angular separation was 2.2° (0.95° in longitude and 1.98° in latitude), corresponding to less than 0.04 au in arc length at 0.9 au. We compute it using the dot product of the two spacecraft position vectors. The CME is fast enough to drive a sheath with a fast forward shock at its front. Shock and sheath properties were analyzed recently by Trotta et al. (2023). In particular, they studied the shocklets associated with the sheath region observed by Wind and, interestingly, they did not observe shocklet signatures at SolO. Their analysis did not extend to the magnetic cloud (MC) region of the CME. The latter corresponded to the magnetic structure being expelled from the corona, where we observe its specific in situ signatures detailed in Section 2.1. Moreover, they did not make use of the fact that, for a time, SolO and Wind were probing different portions of the MC at the same time. It is this "gap" which we wish to bridge in the present work. With multiple spacecraft probing the MC at different locations at the same time, one can determine the instantaneous properties of the MC by combining measurements taken by both spacecraft (Regnault et al. 2023a).

The layout of the paper is as follows. In Section 2, the CME properties when close to the Sun and the heliospheric context in which the CME propagated are introduced. In Section 3, we compare the properties of the magnetic field profile inside the MC at SolO and at Wind. In Section 4, we combine both profiles to obtain the instantaneous properties of the CME. In Section 5, we compare what would have been the forecasted properties at Wind given those at SolO in the context of space weather with actual measurements at Wind. Finally, in Section 6, we discuss our findings and draw our conclusions.

2. Overview of the in Situ Measurements for the 2021 November 3–5 Coronal Mass Ejection

2.1. Magnetic Cloud Boundaries and Coronal Mass Ejection Coronal Counterpart

The CME discussed in this article was measured in situ starting on 2021 November 3. Figure 1, from top to bottom, shows the position of the spacecraft in Stonyhurst coordinates, the magnetic and plasma (density, temperature, and speed of the protons) measurements along with the fast magnetosonic speed (described later in this section), and the proton-β (thermal pressure over magnetic pressure; Richardson & Cane 1995; Wang et al. 2005) measured by SolO (left) and Wind (right) at the time of the passage of the CME. Respectively, for the magnetic and plasma measurements at SolO, we use the magnetometer (MAG; Horbury et al. 2020) and SWA (Owen et al. 2020) instruments, and for Wind we use the Magnetic Field Investigation (Lepping et al. 1995), Solar Wind Electron (SWE; Ogilvie et al. 1995), and 3-D Plasma and Particle Investigation (3DP; Lin et al. 1995) for the temperature.

The present work focuses on the study of the MC part of the CME. MCs are characterized by (i) an above average magnetic field strength, (ii) a smooth and large rotation of the magnetic field vector, and (iii) a low proton-β (Burlaga et al. 1981). However, using only these criteria, the MC start time at Wind would be hard to define. We thus decide to start the MC where the speed profile starts to decrease monotonically following a linear trend, as expected for an expanding MC (Burlaga & Behannon 1982; Farrugia et al. 1993; Gulisano et al. 2010). The end of the MC is chosen to be when the proton-β increases suddenly along with a drop in the magnetic field strength at both spacecraft. A more detailed description of the MC properties can be found in Section 2.2. Using these boundaries, the MC starts on 2021 November 4, 07:09 UT and ends on 2021 November 4, 19:38 UT at SolO. For Wind, the MC starts on 2021 November 4, 12:06 UT and ends on 2021 November 5, 04:14 UT. MC boundaries are shown in magenta for SolO and orange for Wind. To show the overlap of the in situ measurements, MC boundaries at Wind appear in a lighter color in the SolO panel (left), and vice versa. We note significant differences (up to a factor of 10) in the temperature measurements between SWE and 3DP instruments within the MC region. For sake of completeness, we plot both time profiles, but since no temperature drop is observed with SWE while there is a clear drop at SolO temperature measurement, we decide to use 3DP to compute the β parameter. We emphasize that such large discrepancies do not occur for the speed or for the density.

The coronal counterpart of this event should have erupted between October 30 and November 1 since a CME typically takes 2–4 days to reach the Earth (Gopalswamy et al. 2001). However, in this time interval five CMEs are observed in both the STEREO/COR and Solar and Heliospheric Observatory/LASCO coronagraphs. Li et al. (2022) studied these CMEs and found, by using the Graduated Cylindrical Shell model (see Thernisien 2011) that only one CME (their CME8) was directed toward Earth. We thus consider that it is this CME of interest that impacted SolO and Wind. This CME propagated at a direction of 20°N and 9°E with respect to the Sun–Earth line, with a tilt angle of −49°. The result of the reconstruction technique can be seen in Figure 2 of Li et al. (2022). We performed the fitting individually with the same reconstruction model and found the same result of the propagation direction within 2°. Given this direction and assuming a self-similar expansion along with a radial propagation, we would expect the CME flank to cross over SolO and Wind.

We inspect EUV and coronagraphic images to determine if there were low-latitude coronal holes or other CMEs launched after the eruption of the CME presented in this study that could cause deflections or impact its propagation (Gopalswamy et al. 2009; Scolini et al. 2022). We found no evidence of any. The CME under study is therefore expected to propagate undisturbed and radially in a relatively "pristine" solar wind.

2.2. Description of the Magnetic Cloud's in Situ Properties

Using the average speed of the MC and its duration, we find that the MC has a radial width of 0.18 au at SolO and 0.25 au at Wind. Liu et al. (2005) fitted the evolution of the observed size of CMEs as a function of distance and found the following propagation law: $S(R) = (0.25 \pm 0.01) \times R^{0.92 \pm 0.07}$, with R the distance from the Sun in astronomical units. With the size at SolO, we then find that the MC at Wind should have a size of 0.21 au, which is smaller than the size we actually measure. This shows that this statistical relationship does not explain the increase in the MC radial size of this event from SolO to Wind. It is important to note that, to the best of our knowledge, the 0.92 power-law index from Liu et al. (2005) is one of the highest that we can find in the current literature. Thus, 0.21 au corresponds to an MC size estimate at Wind from SolO measurements on the higher end. This could be due to the different trajectories of the spacecraft through the MC even though they are close to each other. This matter is discussed in more detail in the rest of the paper.

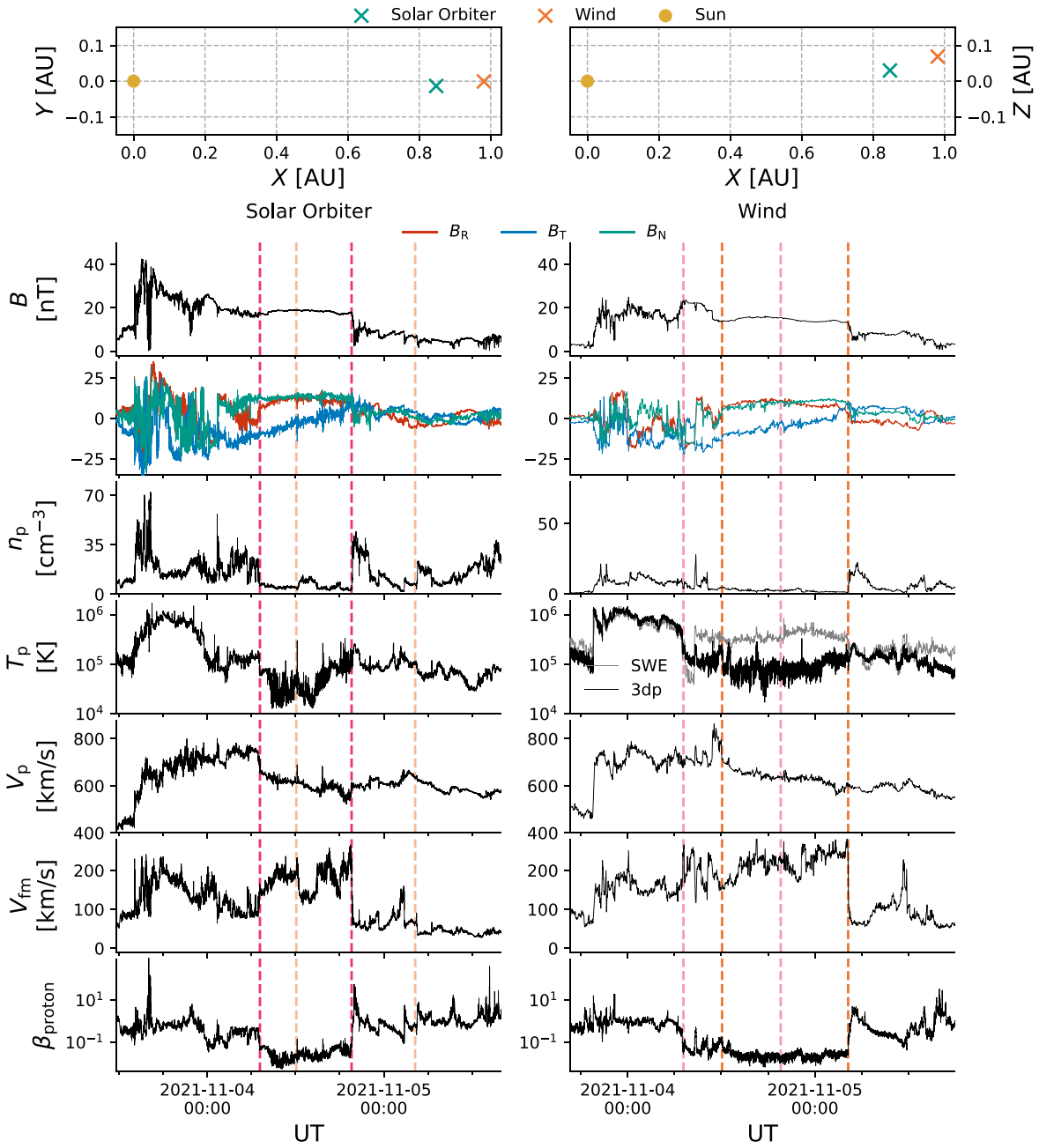

Figure 1. Spacecraft positions and magnetic and plasma measurements at Solar Orbiter (left) and Wind (right) during the passage of the 2021 November 3–5 CME. From top to bottom: position of the spacecraft in Stonyhurst coordinates, *X*–*Y* plane (left) and *X*–*Z* plane (right), the magnitude of the magnetic field (in nanotesla), its components (in nanotesla) in RTN coordinates, the proton density (in cubic centimeters), the temperature (in kelvin, measured by the SWE and 3DP instruments), the bulk speed (in kilometers per second), the fast magnetosonic speed (in kilometers per second) and the proton-β. MC boundaries are delineated in magenta for SolO and orange for Wind. The vertical axes of the SolO and Wind panels are on the same scale.

The sixth row of Figure 1 shows the fast magnetosonic speed $V_{\rm fm}$ at SolO and at Wind. It corresponds to the maximum speed that fast magnetosonic waves propagate in a magnetized plasma, defined as follows:

$$v_{\rm fm}^2 = v_{\rm a}^2 + c_s^2, \quad (1)$$

where $v_{\rm a}$ is the Alfvén speed and c_s is the speed of sound. We take $\gamma = 5/3$ to derive the sound speed.

The quantity $v_{\rm fm}$ corresponds to the fastest way for information to propagate from one point in the MC to another. We compute its average value in the MC at both spacecraft and find 175 km s^{-1} at SolO and 219 km s^{-1} at Wind. We find here that $v_{\rm fm}$ increases from SolO to Wind, which is not what we expect since Wind is further from the Sun and $v_{\rm fm}$ is expected to decrease with distance in the solar wind. This increase is due to the fact that the average density of the MC at Wind is much lower than at SolO (5.7 versus 2.6 cm^{-3}, respectively) while the average magnetic field is similar (18.2 versus 14.5 nT).

The shock time observation is 14:04 UT at SolO and 19:35 UT at Wind on the 2021 November 3 (Trotta et al. 2023), which leads to a time delay of 5 hr and 31 minutes between SolO and Wind. Within that time, fast magnetosonic waves have time to travel between 0.02 and 0.03 au (depending on whether the speed used is based on SolO or Wind measurements), which is much less than half of the estimated MC size.

We use the shock arrival time to determine the delay of the CME between SolO and Wind rather than the MC boundaries because the shock is the easiest feature to locate and thus give the most accurate time-delay estimate.

These considerations will be important when determining whether the discrepancies in the magnetic field highlighted in Section 3.1 can be explained only with time evolution or if other reasons, such as the angular separation between the spacecraft, need to be invoked.

3. Comparing the Magnetic Cloud Properties

In this section, we compare the velocity and magnetic field measurements made by the two spacecraft in the MC region to see how different they are at two spacecraft that have an angular and radial separation of only 2.2° and 0.13 au. In order to establish how much of any discrepancy can be attributed to instrumental effects, we compute the average difference between magnetic field and speed measurements made at Wind and SolO for small separations. This is presented in the Appendix. To the best of our knowledge, such a cross-calibration of SolO with L1 measurements has not been published. In summary, when SolO and Wind are separated by less than 0.01 au, the magnetic field measurements (the magnitude and the T and N components) differ (on average in absolute value) by 0.4 nT, the B_R component by 0.5 nT, and the speed by 5.18 km s^{-1}. Therefore, any difference in the speed or in the magnetic field that may be found during this event which significantly exceeds these values cannot be fully explained by instrumental effects.

3.1. Magnetic Field Time Profile

Figure 2 shows the magnetic field and velocity and their respective components measured by Wind and at SolO. The left column of Figure 2 shows the magnetic field strength and its components in radial–tangential–normal (RTN) coordinates when no time shift is applied to the data. The right column shows the same parameter but plotted as a function of the time normalized to the MC duration. The left column highlights the strong time overlap between the profiles measured at SolO and Wind, while the right column puts emphasis on the differences in the components of the magnetic field profiles measured by both spacecraft, which we describe now.

A stronger average magnetic field strength is measured at SolO than at Wind, which is somewhat expected due to the expansion of the MC during its propagation from SolO to Wind. The average magnetic field in the MC is 18.2 nT at SolO and 14.5 nT at Wind. The evolution of the magnetic field as a function of the distance from the Sun is often described by a power law $B(r) \propto r^{-\alpha}$, with $\alpha = 1.3$–1.8 (Leitner et al. 2007; Winslow et al. 2015; Davies et al. 2021a). Using the two positions of the spacecraft and the average magnetic field at both spacecraft, we find that $\alpha \sim 1.6$, which fits within the observation range of previous statistical studies. Both magnetic field strength profiles are approximately flat, in particular when looking with the y-scale used in Figure 1.

B_R shows a similar shape at both spacecraft. However, while both B_R profiles start at the same value at the MC front, they start to differ measurably close to the MC center. At the MC rear, they differ by about ∼4 nT. A smooth rotation of B_T is measured at both spacecraft, as expected for two spacecraft with such low angular separations (Lugaz et al. 2018). Under the flux-rope paradigm, the smooth rotation along the T direction suggests a highly inclined flux rope (with the axis roughly perpendicular to the ecliptic plane). We also find that this component of the magnetic field is similar at both spacecraft, with a slight shift toward lower values at Wind. B_N is the component that shows the strongest discrepancies when comparing measurements made by both spacecraft. While SolO measures a B_N approximately constant around 12.5 nT, B_N is found to start at about 6 nT and almost constantly increases at Wind, reaching about 10 nT close to the MC rear. This is a difference of about 50% in B_N for the two spacecraft separated by less than 0.13 au. Assuming the magnetic field components also follow a power law, this decrease of B_N corresponds to a power-law index $\alpha_N > 4$, which is highly unrealistic given constraints on magnetic field conservation and evolution. This is further discussed in Section 5.

The discrepancies discussed above can be interpreted as a physical phenomenon occurring within ∼5 hr and 31 minutes (the time delay between the shock observations at the two spacecraft), which can significantly change the magnetic field properties, such as magnetic reconnection or relaxation of the MC after being compressed at the rear. This point is discussed in further detail in Section 3.3. It can also be interpreted as the effect of the angular separation, although small, between the spacecraft. This would suggest that 2.2° is enough of a separation to result in significant changes in the magnetic field profiles. Lugaz et al. (2018) studied the correlation of the magnetic field strength profile observed by ACE and Wind while separated by different angles around 0.5°–1°. Extrapolating their results, they found that the magnetic strength profile correlation between the two spacecraft reaches 0 when the angular separation becomes as large as 15°–20°. We emphasize that an angular separation of 5°–10° is often considered as a "good" radial alignment (Good et al. 2019; Salman et al. 2020), but we show here that significant discrepancies appear even for separations as small as ∼2°. As discussed further below, under the assumption that MCs are twisted flux ropes with an axial invariance, most of the angular separation between SolO and Wind occurs along the flux-rope axis, i.e., the differences between SolO and Wind measurements are expected to be extremely small unless there is no axial invariance of the magnetic field over scales of 2°.

3.2. Velocity Time Profile

We now address the velocity differences, as highlighted in the fifth panel of Figure 1, to compare the velocity profiles at SolO and Wind. The MC is faster at Wind than at SolO, which is somewhat unexpected. The center speed of the MC is 637 km s^{-1} at Wind and 604 km s^{-1} at SolO. If both spacecraft probe a similar portion of the CME, which is expected to be true for small angular separations, this suggests an acceleration of the CME from SolO to Wind. This is not expected because CMEs that are faster than the solar wind slow down as they propagate due to the drag caused by the solar wind (Vršnak et al. 2013). In this case, the solar wind before the CME at SolO is slower by ∼150 km s^{-1} than its MC center speed, which indicates that the CME should decelerate instead of accelerate, based on our current understanding of CME–solar wind interaction. At Wind, the solar wind before the CME is slower by ∼120 km s^{-1}. Therefore, the apparent acceleration cannot be explained by currently existing models of CME propagation and CME–solar wind interaction, and another explanation, such as the effect of the angular separation, needs to be invoked.

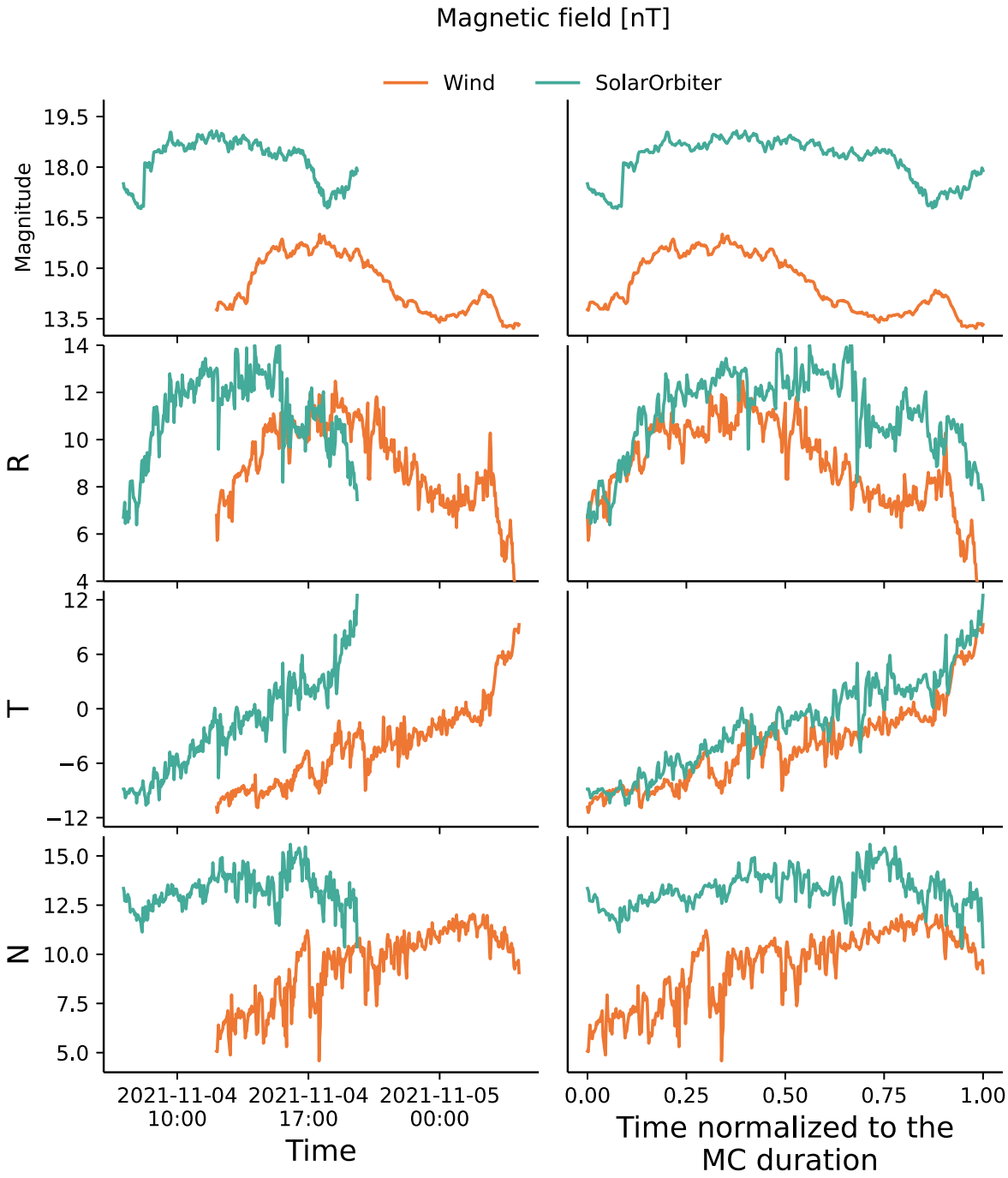

Figure 2. Magnetic field (in nanotesla) strength and its components in RTN coordinates at Wind (orange) and SolO (green) as a function of time (left panel) and time normalized to the MC duration (right panel).

The T and N components of the velocity (not shown) are close to 0 km s^{-1} on average (<10 km s^{-1}) at both spacecraft. Thus, the V_R ($\sim V_{mag}$) profile shows a typical almost monotonic decrease at both spacecraft. These measurements thus suggest that the bulk motion of the MC is locally approximately radial, at least during the duration of the passage of the CME over the spacecraft. The lack of nonradial flows and its consequences for CME expansion were recently discussed in Al-Haddad et al. (2022), and the measurements here are consistent with the findings from this study. Overall, nonradial propagation and complex expansion (which would result in nonradial flows) cannot be invoked to explain the differences between the two spacecraft.

In addition, the bulk motion of the plasma deduced from the speed profile is not consistent with the time delay in the CME arrival at SolO and Wind. The time delay of the MC front between Wind and SolO is only about 4 hr. However, if the MC front does propagate radially, based on the speed measured and the separations between the spacecraft, it would take more than 8 hr to travel 0.13 au (heliocentric distance separation between SolO and Wind) at about 650 km s^{-1}. The differences in the speed as well as the B_N component of the magnetic field inside the MC point toward spatial differences in the MC properties due to the small angular separation between SolO and Wind. We discuss this further in the next section.

3.3. Regarding the Origin of the Discrepancies in the Measurements between Solar Orbiter and Wind

In Sections 3.1 and 3.2, we showed that Wind and SolO measured different MC magnetic and velocity properties. In particular, the magnetic field components (specifically B_N) suggest a change in the MC structure and the velocity profiles suggest an acceleration of the MC. A possible explanation for these discrepancies could be an interaction with the solar wind (e.g., as discussed in Scolini et al. 2022). For instance, a fast solar wind stream could catch up the MC rear, compress it and could also result in a bulk acceleration of the MC. However, no compression signatures are observed at the rear of the MC, such as increased magnetic field strength, density, and temperature. Moreover, an MC being compressed from the rear would typically show an asymmetric magnetic field profile at SolO or Wind, which is not observed. While there is a small rise of the speed close to the rear of the MC, a fairly monotonic decrease of the speed is measured at both spacecraft. If a solar wind stream was pushing the MC from behind, the V_{mag} profile would exhibit a gradient reversal. The speed profile after the end of the MC shows a continuation of the decrease at Wind (see Figure 1), not consistent with a high-speed stream behind the MC.

For this event, there is an increase of the density up to 40 cm^{-3} at SolO and 20 cm^{-3} at Wind compared with the 2–4 cm^{-3} inside the MC (see Figure 1). However, we do not observe significantly faster flows than the MC center speed nor heated plasma at the rear of the MC. We thus do not find any clear signs of compression of the plasma.

In addition, the very short time (~5.5 hr) between the MC observations allows us to rule out time evolution as the main contributor to the observed discrepancies. Indeed, according to the speed of fast magnetosonic waves described in Section 2.2 , waves only have time to travel 0.03 au of the MC, as we discussed in Section 2. However, it is clear from the data shown in Figure 2 that discrepancies in the magnetic field strength profile between the MC at SolO and at Wind are not just contained in the last 0.03 au but rather in about the last half of the MC for B_R and for almost all the MC for B_N, which corresponds, respectively, to a length of 0.09 and 0.18 au at SolO.

Another candidate to explain the differences would be reconnection occurring in the MC. However, this process is often very local and thus is unlikely to explain the discrepancy over such a large part of the MC (half of its radial size). Moreover, we do not observe any reconnection signatures (such as jets of fast plasma and/or enhanced temperatures, or pairs of shocks) in the MC (Owens 2009; Xu et al. 2011).

To conclude, we have shown in this section that the most commonly advanced reasons to explain the discrepancy in the properties of the MC at Wind and at SolO are not consistent with the timing of the CME at both observations, neither with the evolution of B_N from SolO to Wind. The type of diagnostic described in this section is made possible mainly because both spacecraft have a radial separation small enough that fast magnetosonic waves do not have time to travel through the full MC part during the ~5.5 hr between the measurements. Since time evolution fails to explain the discrepancies we observe, such effect is likely produced from the variations of the MC properties on scales as small as ~0.03 au, which has almost never been explored with simultaneous measurements.

4. Instantaneous Expansion Speed

In Section 3, we have described measurable differences between the magnetic field and velocity in situ profiles measured at SolO and at Wind for an MC measured at small angular separations and moderate radial separations. In this section, we perform a thought experiment to emphasize the impact of a 2.2° angular separation on the MC properties. This approach involves demonstrating that the assumption under which both spacecraft observe the same portion of the CME leads to inconsistencies in the quantification of the MC expansion between the standard estimation using a single in situ profile and the instantaneous expansion speed. The estimate of the instantaneous expansion speed is made possible thanks to the specific spacecraft configuration when the CME was observed. To the best of our knowledge, this is the first report of such an estimate through in situ measurements only.

MC expansion speed has often been defined using the following formula (e.g., Owens et al. 2005; Gulisano et al. 2010; Gopalswamy et al. 2015):

$$V_{exp} = \frac{V_{front} - V_{back}}{2}. \quad (2)$$

This formula assumes that all the change in the MC speed profile is due to the expansion of the MC. That is to say, the MC does not significantly accelerate nor decelerate during the time the CME passes over the spacecraft. Under the same assumption, the expansion speed is sometimes defined using the slope of the speed profile during the part of the event for which the speed can be reasonably approximated by a linear function (Gulisano et al. 2010; Lugaz et al. 2020). Again, any bulk acceleration or deceleration shall affect the calculation of the expansion speed.

We perform a linear fit to the MC speed profiles at both spacecraft through the entire MC duration as the speed is close to linearly decreasing. Using the result of this fit, we find the expansion speed at Wind and SolO to be 43 and 41 km s^{-1}, respectively, which is a consistent value between the two spacecraft and also a typical value found in the literature: Gopalswamy et al. (2015) found an average expansion speed for solar cycles 23 and 24 of 51 and 25 km s^{-1}, respectively. With an expansion speed of 43 km s^{-1}, the MC size that was 0.18 au at SolO should increase by 0.007 au when it reaches Wind, which would result in a significantly smaller size than the 0.25 au we calculate from in situ measurements at Wind. We thus find that the measured expansion at SolO cannot explain the increase in size from SolO to Wind. One reason could be that the assumption that the MC speed is constant during the time the CME passes the spacecraft is not justified.

Using the specific spacecraft configuration during the passage of the MC, we can estimate an instantaneous expansion speed. When SolO is probing the center of the MC, Wind is probing its front, as the radial separation of the two spacecraft of 0.13 au is approximately equal to half the MC size at Wind (see also left panel of Figure 2). We thus have a measurement of the speed at the MC front and at its center *at the same time*. We are then able to compute an instantaneous expansion speed combining measurements made by SolO and by Wind with the following formula:

$$V_{exp_{inst}} = V_{front_{Wind}} - V_{center_{SolO}}. \quad (3)$$

This is summarized in Figure 3, which shows the speed profile at SolO and Wind in green and orange, respectively. No

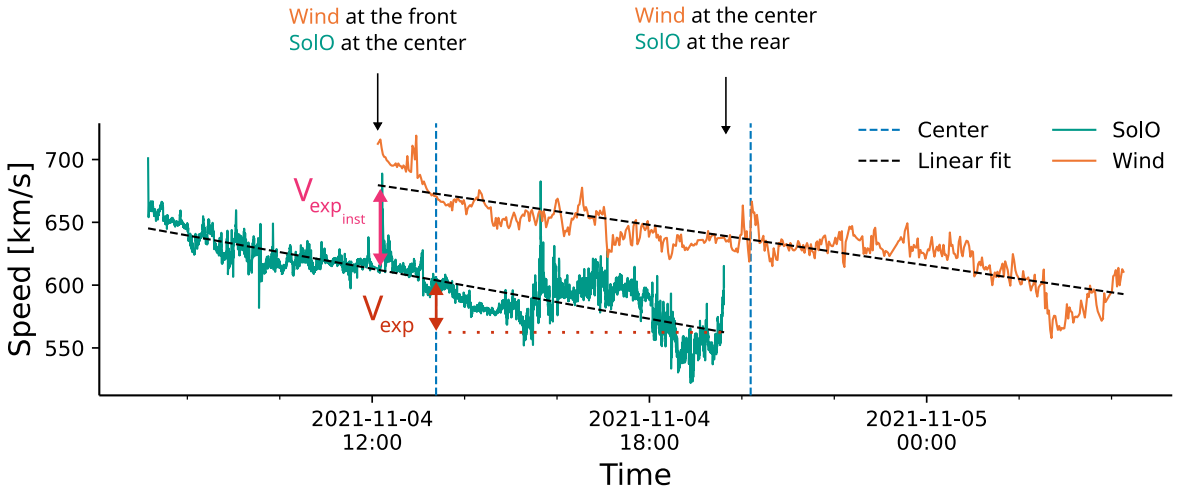

Figure 3. Schematic of the measurement of the instantaneous expansion speed.

time shifting is applied to highlight the instantaneous nature of the measurements at SolO and Wind for about half of the MC duration. Blue dashed lines show the center in time of the MC at both spacecraft. The center speed is assumed to be the speed at the central time of the fit, defined as the cruise (or bulk) speed in Owens et al. (2005).

We now compute the instantaneous expansion speed $V_{\mathrm{exp_{inst}}}$. We use both linear fits of the speed and take the difference during the overlapping time to obtain a value that starts at 68 and increases up to 78 km s^{-1}. On average, we thus obtain $\bar{V}_{\mathrm{exp_{inst}}} = 73$ km s^{-1}, which is 1.7 times the expansion speed calculated using a single speed profile in the MC. This gap is greater than the average absolute difference between the measurements made of the bulk velocity described in the Appendix (5.18 km s^{-1}), and is thus significant. Using this instantaneous expansion speed, the increase in size from SolO to Wind would then be 1.7 times the one we find from a single velocity profile, i.e., 0.012 au. This leads to a predicted size at Wind of 0.192 au, which is still significantly smaller than the 0.25 au that is measured at this location.

Let us now consider the broader scope of the global study rather than focusing solely on the thought experiment conducted in this section. This result could indicate that the MC is accelerating when passing over SolO and Wind, which flattens the "normal" speed profiles, reduces their slopes, and thus decreases the expansion speed we infer from them. This is also consistent with the increased center speed observed at SolO and Wind. However, in the absence of clear compression signatures (see Section 3.3) of the MC at both spacecraft or a high-speed stream behind the MC, the origin of such acceleration at about 0.8–1 au remains mysterious, and spatial (rather than temporal) variations within the MC, even at scales of 2.2°, are a more likely explanation. In addition, this increase of the expansion speed is not enough to explain the large increase of the size from SolO to Wind highlighted in Section 2.2.

This explains why we interpret this result as the fact that the assumption under which both spacecraft probe the same portion of the MC does not hold, even when spacecraft are within 2.2° from each other. To summarize, the results presented in this section highlight how impactful a 2.2° angular separation between two spacecraft can be on MC properties deduced from in situ profiles.

5. Impact of the Angular Separation on the Forecasted Properties at 1 au

In the context of space-weather analysis, SolO was in a very good position (i.e., an almost perfect radial alignment and upstream of L1) to perform forecasting of the CME properties or its arrival time at the Earth. It is this exercise that we perform in this section. Note, however, that we use science-level data from SolO, which differ from the real-time data streams, so this is an exercise of hindcasting rather than forecasting.

The shock arrival time is computed using the speed right after the shock, as we can observe in Figure 1. At SolO, the front of the sheath has a speed of about 680 km s^{-1}. Thus, the shock can be forecasted to take 7 hr and 58 minutes to travel the 0.13 au separating SolO and Wind. In reality, it took only about 5 hr and 31 minutes. Such an estimate would then have provided an arrival time that was 2.5 hr too late when the MC was just 5.5 hr away, which corresponds to a relative error of 45%. This is a really notable error given the short distance between SolO and the Earth when the CME was observed.

In addition, the CME speed would be underestimated by at least 40 km s^{-1}, and by even more if the effect of the drag on the CME speed is taken into account. In order to have a rough estimate of how much the CME would have decelerated from the heliocentric distance of SolO to that of Wind due to the drag effect, we use the Drag-Based Model (DBM; Vršnak et al. 2013). This model is often used to estimate CME arrival time and impact speed. As inputs, the CME coronagraphic speed of 1235 km s^{-1} as found in Li et al. (2022) and an asymptotic solar wind speed of 450 km s^{-1} as measured in Section 1 before the CME arrival time are used. The drag parameter Γ is determined to obtain a CME speed of about 670 km s^{-1} at the location of SolO (corresponding to the observed MC front speed). We find that a drag parameter of $0.24\,10^{-7}$ km^{-1} produces an impact speed of 669 km s^{-1}. This Γ value fits within its typical range described in Vršnak et al. (2013). According to this model, the CME decelerates by about 30 km s^{-1} from SolO to Wind due to the drag. Combining the measured speed increase with the expected speed decrease, the total underestimation using SolO measurements is of about 70 km s^{-1} for the CME front speed.

We note that with this Γ value, the DBM model predicts a CME arrival time on 2021 November 3, 15:00 UT, which is a mismatch of more than 16 hr with the actual observations.

Further, increasing Γ to reduce this mismatch leads to a CME speed of about 500 km s^{-1} at SolO, which is much lower to the one measured.

On top of the arrival time and speed estimates, the prediction of the geoeffectivity of the CME could have been significantly off, too. Indeed, the north–south component of the magnetic field ($\sim B_N$) is the most important for determining the geoeffectivity of a CME. A large and prolonged southward-oriented magnetic field is the most geoeffective magnetic field configuration (Gonzalez & Tsurutani 1987). While the B_N component is mostly positive (northward magnetic field) during this MC, we discuss the difference between the two spacecraft under the assumption that such differences would have applied, even if B_N had been negative.

While the magnetic field strength of the MC front at both spacecraft matches well, the B_N values differ by about 6 nT ($\sim$12.5 nT at SolO and $\sim$6.5 nT at Wind). If we take into account the expansion of the magnetic field from SolO to Wind, and with $\gamma = 1.8$, we would expect a decrease of B_N from SolO to Wind of 2.4 nT, and there is still an unexplained difference of 3.6 nT. This is a 55% relative error on the geoeffective component of the magnetic field of MC that we would have forecasted at the Earth. Again, since the CME had a northward magnetic field within the MC, it was not likely to be geoeffective, in any case, but such relatively large differences in the B_N component of the magnetic field from two spacecraft in close proximity is worrisome for space-weather forecasting using upstream monitors. In summary, even if the MC was only 0.13 au away and with a 2.2° angular separation, current models would have failed to accurately predict the speed, the arrival time at Wind, and the magnitude of the B_N component of the magnetic field at Earth, with errors of 40%–50% for lead times of $\sim$4.5 hr.

6. Discussion and Conclusion

In this paper, we have shown that even when two spacecraft have an angular and radial separation of 2.2° and 0.13 au, respectively, significant discrepancies in their magnetic and speed parameter profiles can exist. The angular separation is very small as compared to the typical angular extent of CMEs seen in coronagraphs (60°; Wang et al. 2011). Such an angular separation corresponds to about 0.03 au in arc length at 0.9 au. Given this small separation, we initially expected both spacecraft to probe the same portion of the CME and thus observe similar features in the in situ profiles. However, some of the magnetic field components are significantly different between the two spacecraft. While the expansion speed is the same at both spacecraft, speed profiles suggest an acceleration of the CME from SolO to Wind. This is indicated both by the increase of the center speed from SolO to Wind and with the flattening of the speed profile inferred by the comparison of the expansion speed with, and without, the effect of the CME temporal evolution. But it is not clear what physical process could cause such an acceleration rather than the expected deceleration due to the drag force exerted by the solar wind. We thus attribute these discrepancies to the effect of the variation of the MC across its cross-section within 2.2° (or an arclentgh of 0.03 au), even though the separation is primarily in the direction of the expected MC axis under the current flux-rope paradigm.

In recent years, researchers have had more opportunities than before to perform multi-spacecraft studies of the same CME by spacecraft separated by 0.2–0.8 au and by 1°–10° while typically assuming that the angular separation has a smaller impact than radial separations. The approach thus assumes that the CME is coherent within these spatial scales. The current work sheds light on the importance of "small" spatial scales (i.e., as small as $\sim$0.03 au of arc length) on the MC properties. Davies et al. (2020) found discrepancies in the results of fitting outputs of the same CME observed in particular by Wind and Juno. At the time of the CME passage, Wind and Juno were radially and angularly separated by 0.24 au and 3.6°, respectively. The time delay between the CME front at both spacecraft in their study was about 20 hr. In this study, we find similar discrepancies but with only about 5 hr of time delay (for the shock and MC front). This clearly highlights that "small" angular separations may have a significant impact on the MC properties as measured by two spacecraft. In fact, for this event, the effect of the small angular separation is clearly larger than the impact of the radial separations between the spacecraft, even though the separation is primarily along the MC axis (i.e., there is limited influence of a different impact parameter).

Moreover, trying to use the CME speed at SolO to hindcast the arrival time at Wind results in a relative error of 45%. According to Riley et al. (2018) and Wold et al. (2018), the typical error for the CME arrival deduced from its coronal properties (potentially coupled with simulations) is 10 hr, which corresponds to a relative error of 13%, taking 3 days as the typical CME transit time. Thus, our findings suggest that local measurements made just 0.13 au ahead and 2.2° off the Sun–Earth line provide, in this case, a worse prediction than when global properties close to the Sun deduced from remote sensing are used. This sheds light once again on the effect of the local nature of the in situ measurements and the need for more multi-spacecraft measurements of the same CME at small separations.

This study presents a case study of a CME with both magnetic and plasma signatures observed by two spacecraft simultaneously in the MC while separated by only 2.2°. The event presented here is almost unique: When searching over more than 2000 CMEs observed over the last 40 yr of data, it was the only event with such a spacecraft configuration along with clear CME signatures with both magnetic and plasma data available. The results found here cannot be generalized to all CMEs, but they raise important questions about the coherence scales of the CME magnetic structures. The coherence scales of CMEs have been estimated recently by Lugaz et al. (2018) and Owen et al. (2020) using in situ measurements, and they found an angle ranging from 4° to 26°. Similarly, Scolini et al. (2023) estimated the coherence scale of CMEs simulated within the EUHFORIA model, and they found up to 45° for the magnetic field strength.

In this work, we find significant changes on much smaller scales than the coherence scales computed in these studies. In fact, the scales described in this paper are almost absent in any CME model that relies on simulations, observations, or theory. For instance, for currently existing numerical models of CME propagation up to 1 au, an angle of 2° typically represents a few grid cells (e.g., van der Holst et al. 2014; Pomoell & Poedts 2018; Török et al. 2018; Liu et al. 2022; Regnault et al. 2023b) even when using nonuniform grids or adaptive mesh refinement techniques (or both) to increase the spatial resolution only where it is needed.

To conclude, this study suggests that current CME models cannot explain discrepancies in the properties of an MC measured by two spacecraft even though they are separated by

an angular separation as small as 2°. The close proximity of the spacecraft along with the speed of fast magnetosonic waves allow us to rule out time evolution as being the main contributor of the observed discrepancies. The lack of sufficiently advanced models (both numerical and theoretical) to describe such small spatial scales can be explained by the limitation of numerical resources (having a higher spatial resolution would be too costly) but also by the paucity of CME observations like the one presented in this study, from which there is lot to learn.

Acknowledgments

F.R., N.A., and W.Y. acknowledge grant Nos. 80NSSC21K0463 and AGS1954983. F.R. and N.A. acknowledge grant No. 80NSSC22K0349. N.L. and F.R. acknowledge grant No. 80NSSC20K0700. B.Z. acknowledges grant Nos. 80NSSC23K1057 and AGS-2301382. C.J.F. acknowledges support from grant No. 80NSSC21K0463 and Wind grant No. 80NSSC19K1293. E.D. acknowledges funding by the European Union (ERC, HELIO4CAST, 101042188). Views and opinions expressed are, however, those of the author(s) only and do not necessarily reflect those of the European Union or the European Research Council Executive Agency. Neither the European Union nor the granting authority can be held responsible for them.

Appendix
Assessing the Calibration between SolO and Wind Measurements

In this section, we compare the measurements made by Wind and SolO data during the SolO flyby close to the Earth (<0.01 au) late 2021 November. Figure 4 shows the magnetic field (top panel), its RTN components (2nd, 3rd, and 4th panels), and the speed (bottom panel) at Wind (green) and at SolO (orange) as a function of time during the flyby. We can see that early on 2021 November 27, the magnetic field quickly increases to ∼100 nT and the speed decreases as slow as ∼40 km s^{-1} in the SolO measurements. This probably corresponds to SolO crossing Earth's magnetospheric boundaries, as these values are not usually reached in normal observation of the solar wind properties close to 1 au. Thus, in order to compare Wind and SolO measurements and not be affected by these artifacts in our calibration check, we remove the data in a 14 hr time window around it. Data points within this time window are shown in gray in Figure 4.

Table 1 shows the mean, median, and maximum absolute difference between the magnetic field strength (and its components) and the speed measured by SolO and Wind along with the standard deviation of the absolute difference. Computing the absolute difference in the magnetic field strength and speed data between Wind and SolO, we find a mean of 0.40 nT and 5.2 km s^{-1} with a standard deviation of 0.34 nT and 5.42 km s^{-1} and a maximum difference of 1.48 nT and 26.37 km s^{-1} for the magnetic field strength and the speed, respectively.

Similarly, we compute the median of the difference, and find 0.30 nT and 3.59 km s^{-1}. These values show that there is a good agreement between Wind and SolO measurements for small separations. We also want to point out that, even if the separation between the two spacecraft is low, it is still nonzero. Assuming that the magnetic field of the solar wind decreases as r^{γ} with

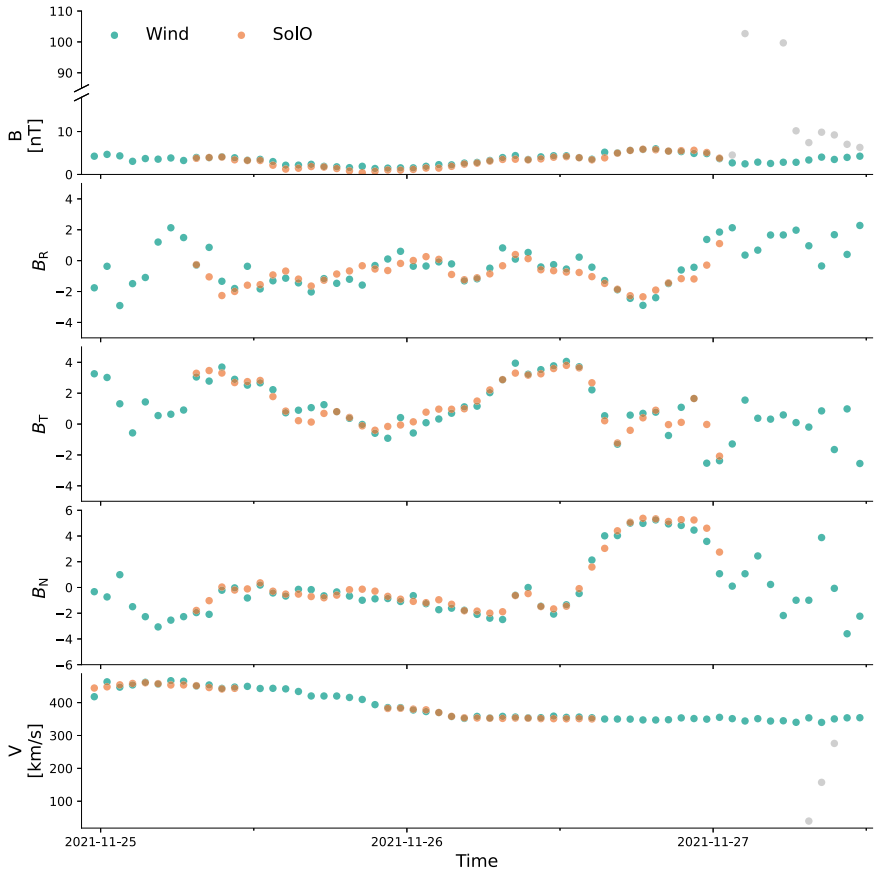

Figure 4. Cross-correlation of the Wind (green) and SolO (orange) hourly binned time series for the magnetic field strength (top panel) and speed (bottom panel) during SolO flyby close to the Earth. Gray points correspond to data not taken into account in the cross-correlation.

Table 1
Mean and Median, Maximum Absolute Error, and Standard Deviation of the Difference between SolO and Wind Measurement When SolO Was Less Than 0.01 au Away from the Earth

Parameter	Mean	Median	Max	σ
B_{mag} (nT)	0.40	0.30	1.48	0.34
B_R (nT)	0.52	0.40	1.91	0.43
B_T (nT)	0.41	0.28	2.51	0.43
B_N (nT)	0.41	0.37	1.68	0.34
V_{mag} (km s^{-1})	5.18	3.59	26.37	5.42

$\gamma = 1.8$–1.9, 0.01 au is enough to see a decrease of 0.1 nT for a magnetic field of 5 nT, which probably contributes to the 0.4 nT average difference of the magnetic field measurements.

ORCID iDs

F. Regnault https://orcid.org/0000-0002-4017-8415
N. Al-Haddad https://orcid.org/0000-0002-0973-2027
N. Lugaz https://orcid.org/0000-0002-1890-6156
C. J. Farrugia https://orcid.org/0000-0001-8780-0673
W. Yu https://orcid.org/0000-0002-2917-5993
B. Zhuang https://orcid.org/0000-0002-5996-0693
E. E. Davies https://orcid.org/0000-0001-9992-8471

References

Al-Haddad, N., Galvin, A. B., Lugaz, N., Farrugia, C. J., & Yu, W. 2022, ApJ, 927, 68
Burlaga, L., Sittler, E., Mariani, F., & Schwenn, R. 1981, JGRA, 86, 6673
Burlaga, L. F., & Behannon, K. W. 1982, SoPh, 81, 181
Burt, J., & Smith, B. 2012, in 2012 IEEE Aerospace Conf. (Big Sky, MT: IEEE), 1
Chiu, M., Von-Mehlem, U., Willey, C., et al. 1998, SSRv, 86, 257
Davies, E. E., Forsyth, R. J., Good, S. W., & Kilpua, E. K. J. 2020, SoPh, 295, 157
Davies, E. E., Forsyth, R. J., Winslow, R. M., Möstl, C., & Lugaz, N. 2021a, ApJ, 923, 136
Davies, E. E., Möstl, C., Owens, M. J., et al. 2021b, A&A, 656, A2
De Lucas, A., Dal Lago, A., Schwenn, R., & Clúa De Gonzalez, A. 2011, JASTP, 73, 1361
Farrugia, C. J., Burlaga, L. F., Osherovich, V. A., et al. 1993, JGRA, 98, 7621
Fox, N. J., Velli, M. C., Bale, S. D., et al. 2016, SSRv, 204, 7
Gonzalez, W. D., & Tsurutani, B. T. 1987, P&SS, 35, 1101
Good, S. W., & Forsyth, R. J. 2016, SoPh, 291, 239
Good, S. W., Kilpua, E. K. J., LaMoury, A. T., et al. 2019, JGRA, 124, 4960
Gopalswamy, N., Lara, A., Yashiro, S., Kaiser, M. L., & Howard, R. A. 2001, JGRA, 106, 29207
Gopalswamy, N., Mäkelä, P., Xie, H., Akiyama, S., & Yashiro, S. 2009, JGRA, 114, A00A22
Gopalswamy, N., Yashiro, S., Xie, H., Akiyama, S., & Mäkelä, P. 2015, JGRA, 120, 9221
Gulisano, A. M., Démoulin, P., Dasso, S., Ruiz, M. E., & Marsch, E. 2010, A&A, 509, A39
Horbury, T. S., O'Brien, H., Carrasco Blazquez, I., et al. 2020, A&A, 642, A9
Kaiser, M. L., & Adams, W. J. 2007, in 2007 IEEE Aerospace Conf. (Big Sky, MT, USA: IEEE), 1
Kaiser, M. L., Kucera, T. A., Davila, J. M., et al. 2008, SSRv, 136, 5
Kilpua, E. K. J., Good, S. W., Dresing, N., et al. 2021, A&A, 656, A8
Leitner, M., Farrugia, C. J., Möstl, C., et al. 2007, JGRA, 112, A06113
Lepping, R. P., Acũna, M. H., Burlaga, L. F., et al. 1995, SSRv, 71, 207
Li, X., Wang, Y., Guo, J., & Lyu, S. 2022, ApJL, 928, L6
Lin, R. P., Anderson, K. A., Ashford, S., et al. 1995, SSRv, 71, 125
Liu, Y., Richardson, J., & Belcher, J. 2005, P&SS, 53, 3
Liu, Y., Shen, F., Yang, Y., & Ma, M. 2022, ApJ, 940, 11
Lugaz, N., Farrugia, C. J., Winslow, R. M., et al. 2018, ApJL, 864, L7
Lugaz, N., Salman, T. M., Winslow, R. M., et al. 2020, ApJ, 899, 119
Lugaz, N., Salman, T. M., Zhuang, B., et al. 2022, ApJ, 929, 149
Möstl, C., Weiss, A. J., Reiss, M. A., et al. 2022, ApJL, 924, L6
Müller, D., St. Cyr, O. C., Zouganelis, I., et al. 2020, A&A, 642, A1
Ogilvie, K. W., Chornay, D. J., Fritzenreiter, R. J., et al. 1995, SSRv, 71, 55
Owen, C. J., Bruno, R., Livi, S., et al. 2020, A&A, 642, A16
Owens, M. J. 2009, SoPh, 260, 207
Owens, M. J., Cargill, P. J., Pagel, C., Siscoe, G. L., & Crooker, N. U. 2005, JGRA, 110, A01105
Pomoell, J., & Poedts, S. 2018, JSWSC, 8, A35
Raouafi, N. E., Matteini, L., Squire, J., et al. 2023, SSRv, 219, 8
Regnault, F., Al-Haddad, N., Lugaz, N., et al. 2023a, ApJ, 957, 49
Regnault, F., Strugarek, A., Janvier, M., et al. 2023b, A&A, 670, A14
Richardson, I. G., & Cane, H. V. 1995, JGR, 100, 23397
Riley, P., Mays, M. L., Andries, J., et al. 2018, SpWea, 16, 1245
Salman, T. M., Winslow, R. M., & Lugaz, N. 2020, JGRA, 125, e2019JA027084
Scolini, C., Winslow, R. M., Lugaz, N., & Poedts, S. 2023, ApJ, 944, 46
Scolini, C., Winslow, R. M., Lugaz, N., et al. 2022, ApJ, 927, 102
Thernisien, A. 2011, ApJS, 194, 33
Török, T., Downs, C., Linker, J. A., et al. 2018, ApJ, 856, 75
Trotta, D., Hietala, H., Horbury, T., et al. 2023, MNRAS, 520, 437
van der Holst, B., Sokolov, I. V., Meng, X., et al. 2014, ApJ, 782, 81
Vršnak, B., Žic, T., Vrbanec, D., et al. 2013, SoPh, 285, 295
Wang, C., Du, D., & Richardson, J. D. 2005, JGRA, 110, A10107
Wang, Y., Chen, C., Gui, B., et al. 2011, JGRA, 116, A04104
Winslow, R. M., Lugaz, N., Philpott, L. C., et al. 2015, JGRA, 120, 6101
Winslow, R. M., Lugaz, N., Scolini, C., & Galvin, A. B. 2021, ApJ, 916, 94
Wold, A. M., Mays, M. L., Taktakishvili, A., et al. 2018, JSWSC, 8, A17
Xu, X., Wei, F., & Feng, X. 2011, JGRA, 116, A05105